



UNIVERSITI PUTRA MALAYSIA

**EFFECTS OF SYNTHESIS METHODS ON THE PHYSICOCHEMICAL PROPERTIES OF
MICRO- AND NANO-SIZED ZINC OXIDE**

ASHKAN KESHAVARZI

FS 2009 32



**EFFECTS OF SYNTHESIS METHODS ON THE PHYSICOCHEMICAL
PROPERTIES OF MICRO- AND NANO-SIZED ZINC OXIDE**

ASHKAN KESHAVARZI

**MASTER OF SCIENCE
UNIVERSITI PUTRA MALAYSIA**

2009



**EFFECTS OF SYNTHESIS METHODS ON THE PHYSICOCHEMICAL
PROPERTIES OF MICRO- AND NANO-SIZED ZINC OXIDE**

By

ASHKAN KESHAVARZI

**Thesis Submitted to the School of Graduated Studies, Universiti Putra Malaysia,
in Fulfilment of the Requirements for Degree of Master of Science**

April 2009



Abstract of the thesis presented to the Senate of Universiti Putra Malaysia in fulfilment of requirement for the degree of Master of Science

**EFFECTS OF SYNTHESIS METHODS ON THE PHYSICOCHEMICAL
PROPERTIES OF MICRO- AND NANO-SIZED ZINC OXIDE**

By

Ashkan Keshavarzi

April 2009

Chairman : Associate Professor Abdul Halim Bin Abdullah, PhD
Faculty : Science

Zinc oxide is an important semiconductor material, which is useful in various applications such as photo-electric devices electronic devices, surface acoustic wave, devices field emitters sensors, ultraviolet lasers and solar cells. With a wurtzite hexagonal phase, ZnO have a direct band gap of 3.37 eV with the larger exciton binding energy (60 meV), possesses a wide range of technological applications including flat panel displays, UV lasers and chemical and biological sensors. Till now, many methods have been developed to synthesize zinc oxide nanocrystals including vapor phase growth, ultrasonic irradiation, hydrothermal, pulsed lased deposition, vapor–liquid–solid process, soft chemical method, electrophoretic deposition, sol–gel process. Depending on the adopted synthesis method, zinc oxide nanocrystals would show various morphologies under different formation mechanisms.



In this work, we studied preparation of ultra fine and nano sized ZnO by four important methods. ZnO nanoparticle, nanorod, nanowire have been successfully synthesized by facile methods like ultrasonic irradiation, sol-gel method, decomposition of Zn substrate and hydrothermal methods.

In our work, three anionic surfactants Cetyl trimethylammonium bromide (CTAB), Tetrabutylammonium bromide (TBAB) and Sodium dodecyl sulfate (SDS) have been used as capping agent in the hydrothermal process. The results demonstrated that structure of the surfactant and its carbonyl chain group is important to crystal growth of the products. SEM and TEM micrograph revealed that nano fiber and ultrafine spherical ZnO prepared in the presence of CTAB and TBAB, but in the presence of SDS, sheet form of ZnO was prepared.

The effect of ultrasonic irradiation was studied on preparation of ZnO. Nanoparticle of ZnO was synthesized after precipitation of zinc nitrate by urea at 90°C with irradiation of waves into the reaction flask for 2h. After heat treat at 350°C, sample was characterized with FT-IR, XRD, SEM, TEM and UV-vis. The results shows the nanoparticles of ZnO are in size range of 50-120nm.

The effect of solvent was studied in this work, too. Ethanol, ethylene glycol and isopropanol were used as solvent in the reaction. In the other hand, characterization of products was shown that morphology and particle size of products was very different and depended to the dielectric constant of the solvents.



Abstrak tesis yang dikemukakan kepada Senat Universiti Putra Malaysia bagi memenuhi keperluan untuk ijazah Master Sains

**KESAN CARA PENYEDIAAN KE ATAS SIFAT-SIFAT FIZIKAL DAN KIMIA
MIKRO DAN SAIZ NANO ZINK OKSIDA**

Oleh

Ashkan Keshavarzi

April 2009

Pengerusi : Profesor Madya Abdul Halim bin Abdulah, PhD
Fakulti : Sains

Zink oksida merupakan bahan semikonduktor yang baru dan penting, di mana ia meluas digunakan dalam pelbagai aplikasi seperti alat-alat fotoelektrik dan elektronik, permukaan gelombang akautik, pengesan alat pemancar, laser ultralembayung dan sel solar. Zink oksida mempunyai jurang tenaga sebanyak 3.37 eV dengan tenaga ikatan pengujian yang besar (60 meV) dan mempunyai fasa wurzite heksagonal. Penggunaannya dalam bidang teknologi termasuk skrin rata, laser UV dan pengesan kimia dan biologi. Pelbagai kaedah telah diusahakan untuk mensintesis zink oksida seperti pembesaran fasa wap, ultrasonik, hidroterma, penempelan hembasan laser, proses wap-cecair-pepejal, kaedah tindak balas perlahan, elektroforetik dan proses sol-gel. Nano kristal zink oksida akan menunjukkan pelbagai morfologi melalui mekanisme pembentukan yang berlainan bergantung kepada kaedah sintesis.

Penyediaan ultrahalus dan nano zink oksida telah dilakukan melalui 6 kaedah yang sesuai dalam kajian ini. Sintesis zarah nano zink oksida, nanorod dan nanowayar telah dilaksanakan melalui kaedah mudah seperti ultrasonik, sol-gel, penguraian substrat zink dan kaedah hidroterma.

Dalam kajian ini, tiga surfaktan anionik iaitu CTAB, TBAB dan SDS telah digunakan sebagai agen penutup dalam proses hidroterma. Keputusan menunjukkan bahawa struktur surfaktan dan rantai kumpulan karbonil sangat penting dalam pertubuhan kristal. FE-SEM dan TEM mikrograf menunjukkan fiber nano dan ultrahalus didapati dalam zink oksida yang disediakan oleh CTAB dan TBAB manakala bentuk kepingan jika SDS digunakan.

Kesan ultrasonik ke atas penyediaan zink oksida juga dikaji. Zarah nano zink oksida telah dihasilkan selepas pemendakan zink nitrat oleh urea pada 90 °C dengan penyinaran gelombang selama 2 jam. Selepas rawatan haba pada 350 °C, sampel yang dihasilkan akan diperihalkan dengan FT-IR, XRD, FE-SEM, TEM dan UV-Vis. Keputusan menunjukkan bahawa zarah nano zink oksida di antara 50-120 nm telah dihasilkan.

Kesan pelarut juga dikaji dalam kajian ini.. Etanol, etilene glikol dan isopropanol telah digunakan sebagai pelarut. Keputusan menunjukkan bahawa morfologi dan saiz zarah produk adalah berlainan dan adalah bergantung kepada pemalar dielektrik pelarut.

ACKNOWLEDGMENTS

I wish to express my foremost appreciation to Associate Professor Dr. Abdul Halim Abdullah and Professor Dr. Zulkarnain Zainal for patiently guiding me through the course of this thesis to its eventual end, enlightening me scientifically and resolving my many technical crises.

I would like to express my thank you to Madam Faridah for helping me operates scanning electron microscopy (SEM) and transmission electron microscopy (TEM) analysis at the Institute Bioscience.

Further thanks are extended to my lab mates Sook Keng, Siew Cheng and special thank to Lee Kian Mun who gave me a lot of support and assistant whenever I need it.

Not least, I am eternally grateful to my father, mother and specially my wife for their ever present love and support, without which I would never have succeeded in my academic endeavors.



DECLARATION

I declare that the thesis is my original work except for the quotations and citations which have been duly acknowledged. I also declare that it has not been previously, and is not concurrently, submitted for any other degree at Universiti Putra Malaysia or at any other institution.

ASHKAN KESHAVARZI

DATE: 21.04.2009



TABLE OF CONTENTS

ABSTRACT	Page iii
ABSTRAKT	V
ACKNOWLEDGMENT	Vii
DECLARATION	iX
LIST OF FIGURES	Xiii
LIST OF ABBREVIATIONS	XV
CHAPTER	
I INTRODUCTION	1
1.1 Zinc Oxide Crystal structure and lattice parameters	2
1.2 Band gap energy	4
1.2.1 Opportunities from band gap engineering	6
1.3 Electrical properties	7
1.4 Optical properties	7
1.5 ZnO nanostructures	8
1.5.1 Nanorods and nanowires	9
1.5.2 Nanobelts	11
1.5.3 Nanosprings and nanorings	12
1.6 Applications of ZnO	15
1.7 Objectives	16
II LITERATURE REVIEW	18
2.1 Thermal decomposition	18
2.2 Solution synthesized methods	19
2.2.1 Hydrothermal and solvothermal method	21
2.2.1.1 Mechanism of crystal growth	22
2.3 Sonochemical synthesis	25
2.3.1 Sonochemical mechanism	26
2.4 Other methods	27
2.4.1 Evaporation-condensation growth	27
2.4.2 Thin film technique	30
2.4.3 PLD method	32
III MATERIALS AND METHODS	38
3.2 Methods	34
3.2.1 Precipitation method	35
3.2.2 Sol-gel method	36
3.2.3 Solvothermal method	37
3.2.4 Thermal decomposition method	37
3.3 Characterization	38



IV RESULTS AND DISCUSSION	39
4.1 Synthesis of ZnO by precipitation via urea hydrolysis	39
4.1.1 Mechanism of the reaction	43
4.1.2 Effect of reaction method on morphology and particle size	43
4.1.3 UV-vis analysis	46
4.2 Synthesis of ZnO by precipitation via NH ₃ addition	47
4.2.1 Particle morphology by FESEM and TEM	47
4.3 Synthesis of ZnO by precipitation via NaOH	52
4.3.1 Possible mechanism	55
4.4 Synthesis of ZnO by Sol-gel method	58
4.4.1 Possible mechanisms of crystal growth	61
4.4.2 Effect of temperature on crystal growth	63
4.5 Synthesis of ZnO by solvothermal method	65
4.6 Synthesis of ZnO by thermal decomposition method	70
4.6.1 Growth mechanism	71
V CONCLUSION	75
RECOMMENDATIONS FOR FURTHER STUDIES	76
REFERENCES	77
BIODATA OF STUDENT	83



LIST OF FIGURES

Figure		Page
1	Wurtzite structure model of ZnO (a) the structure model of ZnO displaying the $\pm(0001)$, $\pm(10\bar{1}\bar{1})$ and $\pm(10\bar{1}1)$ polar surfaces (b).	4
2	The LDA band structure of bulk wurtzite ZnO calculated using dominant atomic self-interaction-corrected pseudopotentials.	6
3	ZnO nanorods grown using gold as a catalyst (a). An enlarged image of the nanorods, showing gold particles at the tips (b).	11
4	TEM images of the as-synthesized ZnO nanobelts, showing uniform morphology.	12
5	Model of a polar nanobelt. Polar surface induced formation of (b) nanoring and nanospiral.	13
6	Formation of the single-crystal nanoring via self-coiling of a polar nanobelt.	15
7	A schematic diagram of the experimental apparatus for growth of oxides nanostructures by the solid–vapor phase process.	28
8	Schematic of a pulsed laser deposition system.	32
9	The XRD pattern of hydrozincite powder prepared by ultrasonic (UM) and conventional heating method (CHM) and JCPDS file pattern of Hydrozincite.	40
10	XRD pattern of heat treated hydrozincite produced in the absence (CHM) and presence (UM) of ultrasonic irradiation and JCPDS file pattern of ZnO.	41
11	FT-IR spectra of hydrozincite as prepared in the (A) absence (CHM) and (B) presence (UM) of ultrasonic irradiation and (C) ZnO produced after heat treatment at 350°C.	42
12	TEM image of hydrozincite prepared in the absence (A1) and presence of ultrasonic irradiation (B1) and relative ZnO prepared after annealing (A2) and (B2).	45
13	Particle size distribution curve of UM and CHM ZnO powders.	45
14	UV–vis reflectance spectra for ZnO powder prepared by ultrasonic and conventional heating method.	46
15	XRD pattern of ZnO prepared in water-ethanol (a), ethylene glycol (b) and water-iso propanol mixtures.	47



16	FESEM Images of ZnO Prepared in aqueous solution ethanol (a), ethylene glycol (b) and isopropanol (c).	49
17	TEM images of ZnO particles prepared in aqueous solutions of ethanol (a), ethylene glycol (b) and isopropyl alcohol (c).	50
18	UV-vis reflectance of ZnO powder synthesized via ethanol, ethylene glycol and isopropanol.	51
19	XRD pattern of the ZnO prepared in the presence of CTAB (a),TBAB (b) and SDS(c).	52
20	FESEM images of ZnO prepared in the presence of CTAB (a), TBAB (b) and SDS (c).	53
21	TEM images of ZnO produced in the presence of CTAB (a), TBAB (b) and SDS (c).	54
22	UV-vis reflectance of ZnO powder synthesized via CTAB (a), TBAB (b), SDS (c).	55
23	Molecular structure of CTAB (a), TBAB (b) and SDS (C).Growth schematic of ZnO fiber near carbonyl chain of CTAB (d).	57
24	XRD pattern of ZnO single nanowires prepared at 70°C (a), 120°C and 170°C.	59
25	FESEM images of ZnO wires prepared in the 70°C (a), 120°C (b) 170°C(c).	60
26	TEM and SEM micrographs of ZnO nanowire formed in 70°C. Image of TEM (a) electron diffraction pattern (ED),(a), SEM image of nanowire (b), and hexagonal cross section of ZnO nanowires (c).	61
27	Possibility of crystal growth direction.	63
28	TEM image of ZnO nanowire as prepared in 120°C (d) and 170°C (e).	64
29	UV-vis spectra of ZnO wires prepared at 70°C (a), 120°C (b) and 170°C(c).	65
30	XRD pattern of ZnO prepared solvothermal method using methanol(a), ethanol (b) and isopropanol (c) as medium reaction.	66
31	FESEM images of ZnO prepared using methanol(a), ethanol (b) and isopropanol (c) as solvent.	67
32	TEM images of ZnO prepared by solvothermal method using methanol (a), ethanol (b) and isopropanol (c) as solvent.	68



33	UV-vis spectra of ZnO powder synthesized via ethanol, ethylene glycol and isopropanol.	70
34	XRD pattern of ZnO fibers prepared after heat treat in nitrogen and compressed air atmosphere (a) after heat treat in compress followed by nitrogen atmosphere (b).	72
35	SEM images of ZnC ₂ O ₄ before heat treat (a) and ZnO after heat treat in nitrogen and compressed air atmosphere (b) after heat treat in compressed air and followed by nitrogen atmosphere (c).	73
36	UV-vis spectra of ZnO wires prepared after heat-treated in nitrogen and compressed air atmosphere (a) after heat treat in compressed air and followed by nitrogen atmosphere (b).	74



LIST OF ABBREVIATION

CTAB	Cetyltrimethylammonium Bromide
DAP	Donor-Acceptor Pair
EELS	Electron Loss Energy Spectroscopy
E_g	Band gap energy
ETMB	Empirical Tight Binding Method
FESEM	Field Emission scanning electron Microscopy
FT-IR	Fourier Transform-Infra Red
HMTA	Hexamethylenetetraamine
JCPDS	Joint Committee of Powder Diffraction Standards
LDA	Local Density Appropriation
LMBE	Laser Phase Beam Epitaxy
LO	Longitudinal Optical
PEG	Poly Ethylene Glycol
PVA	Poly vinyl Alcohol
SDS	Sodium Dodecyl Sulfate
TBAB	Tetrabutylammonium Bromide
TEM	Transmission Electron Microscopy
UPS	Ultra violet Photoelectron Spectroscopy



UV	Ultraviolet
VLS	Vapor Liquid Solid
XRD	X-ray Diffraction
ZnO	Zinc Oxide



CHAPTER I

INTRODUCTION

Recently, zinc oxide (ZnO) has attracted much attention within the scientific community as a future material. This is however, somewhat of a misnomer, as ZnO has been widely studied since 1935 by Bunn, with much of our current industry and day to day lives critically reliant upon this compound. The renewed interest in this material has arisen out of the development of growth technologies for fabrication of high quality single crystal and epitaxial layers, allowing for the realization of ZnO based electronic and optoelectronic devices.

ZnO exhibits a direct band gap of 3.37 eV at room temperature with a large exciton binding energy of 60 meV. ZnO has several advantages over GaN in this application. The most important being its larger exciton binding energy and ability to grow single crystal substrates. The strong exciton binding energy, which is much larger than that of GaN (25eV) and the thermal energy at room temperature (26meV), can ensure an efficient exciton emission at room temperature under low excitation energy. Other favorable aspects of ZnO include its broad chemistry leading to many opportunities for wet chemical etching, low power threshold for optical pumping, radiation hardness and biocompatibility. Together, these properties of ZnO make it an ideal candidate for a variety of device ranging from sensors through ultraviolet laser diodes and nanotechnology based devices such as displays.



As research into ZnO continues, difficulties such as the fabrication of p-type ZnO that have so far stalled the development of devices, are being overcome (Tsukazaki *et al.*, 2005).

1.1 Zinc Oxide Crystal structure and lattice parameters

At ambient pressure and temperature, ZnO crystallizes in the wurtzite structure. This is a hexagonal lattice, belonging to the sublattices of Zn^{2+} and O^{2-} , such that each zinc ion is surrounded by a tetrahedron of O^{2-} ions, and vice-versa. This tetrahedral coordination gives rise to polar symmetry along the hexagonal axis. This polarity is responsible for the number of properties of zinc oxide, including its piezoelectricity and spontaneous polarization, and is also a key factor in crystal growth, etching and defect generation. The four most common face terminations of wurtzite ZnO are the polar Zn terminated (0001) and O terminated (000 $\bar{1}$) faces and non polar (11 $\bar{2}$ 0) (*a*-axis) and (10 $\bar{1}$ 0) faces which both contain an equal number of Zn and O atoms. The polar faces are known to possess different chemical and physical properties, and the O terminated face possesses a slightly different electronic structure to the other three faces. Additionally, other surfaces and the (1010) surface are found to be stable; however (11 $\bar{2}$ 0) face is less stable and generally has a higher level of surface roughness than its counterparts.

Aside from causing the inherent polarity in the ZnO crystal, the tetrahedral coordination of this compound is also a common indicator of sp^3 covalent bonding. However; the Zn-O bond also possesses very strong ionic character, and thus ZnO lies on the border line between being classed as a covalent and ionic compound, with an ionicity of $f_i=0.616$.



The lattice parameters of hexagonal unit cell are $a = 3.2495\text{\AA}$ and $c=5.2069\text{\AA}$, and density is 5.605 cm^{-3} . In an ideal wurtzite crystal the axial ratio c/a and the u parameter (which is a measure of the amount by which each atom is displaced with respect to the next along the c - axis) are correlated by the relationship $uc/a = (3/8)^{1/2}$ where $c/a = (8/3)^{3/2}$ and $u = 3/8$ for an ideal crystal. ZnO crystals deviate from this ideal arrangement by changing both of these values. This deviation occurs such that tetrahedral distances are kept roughly constant in the lattice.

The structure of ZnO can be simply describe as a number of alternating planes composed of tetrahedral coordinated O^{2-} and Zn^{2+} ions, stacked alternatively along the c axis (Figur1). The tetrahedral coordination in ZnO results in non central symmetric structure and piezoelectricity. Another important characteristic of ZnO is the polar surface. The most common polar surface is the basal plane. The oppositely charged ions produce positively charged Zn-(0001) and negatively charged $000\bar{1}$ polar surface, resulting in a normal dipole moment and spontaneous polarization along the c axis. Another polar surface is the $\{01\bar{1}1\}$. By projecting the structure along $[1\bar{2}10]$, as shown in (Figur1), beside the most typical $\pm (0001)$ polar surface that are terminated with Zn and O, respectively, $\pm (10\bar{1}1)$ and $\pm (10\bar{1}\bar{1})$ are also polar surfaces. The $(10\bar{1}1)$ type surfaces are not common for ZnO, but they have been observed in nanohelical structure found recently (Wang *et al.*, 2004). The charges on the polar surfaces are ionic charges, which are non transferable and non flowable. Because the interaction energy among the charges depends on the distribution of the charges, the structure is arranged in such a

configuration to minimize to electrostatic energy. This is the main driving force for growing the polar surface dominated nanostructures.

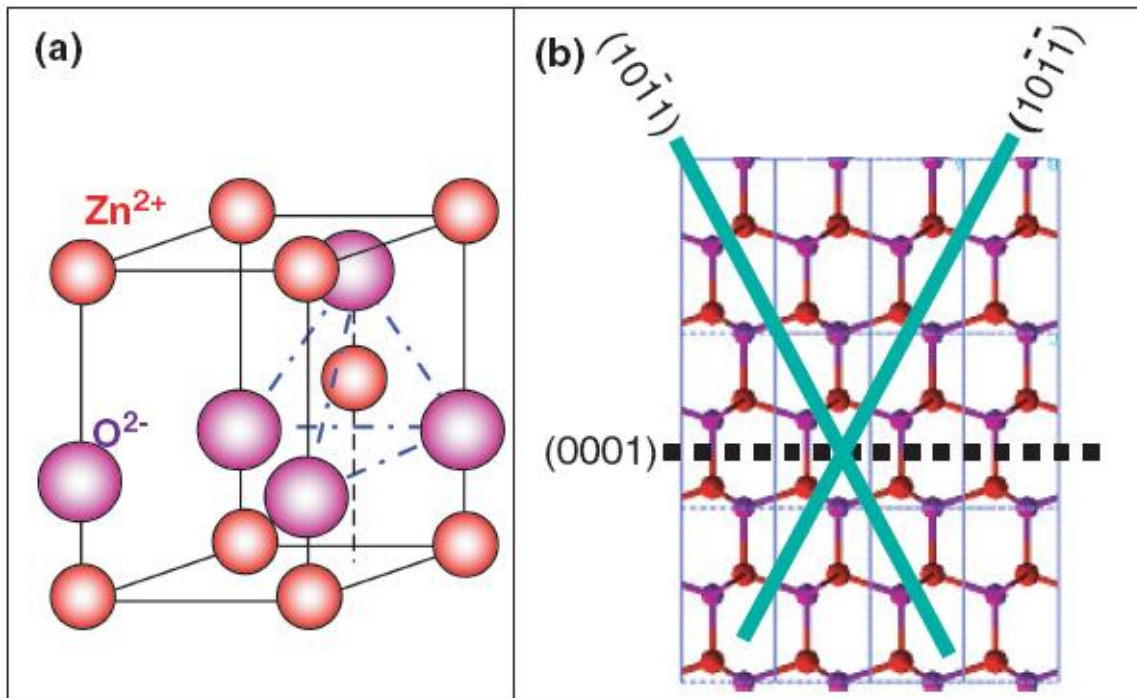


Figure 1:(a) Wurtzite structure model of ZnO (b) The structure model of ZnO , displaying the $\pm(0001), \pm(10\bar{1}1)$ and $\pm (10\bar{1}1)$ polar surfaces. Zinc oxide bulk, thin films and nanostructures processing, properties and applications

1.2 Band gap energy

The electronic band structure of ZnO has been calculated by a number of groups (Jaffe *et al.*, (2000), Usuda and Hamada *et al.*, (2002)) .The results of band structure calculation using the Local Density Appropriation (LDA) and incorporating atomic self-interaction corrected pseudopotentials to accurately account for the $Zn3d$ electrons is shown in Figure 2. The band structure is shown along high symmetry lines in the hexagonal Brillouin zone. Both the valence band maxima and the lowest conduction

band minima accrue at the Γ point $K=0$ indication that ZnO is direct band gap semiconductor. The bottom 10 bands correspond to Zn $3d$ levels. The next 6 bands from -5 eV to 0 eV correspond to O $2p$ bonding state. The first two conduction band states are strongly Zn localized and correspond to empty Zn $3s$ levels. The higher conduction bands are free electron like. The O $2s$ bands associated with core like energy states accrue around -20 eV. The band gap as determined from this calculation is 3.77 eV. This correlates reasonably well with the experimental value of 3.47 eV, and is much closer than the value obtained from standard LDA calculations, which tend to underestimate the band gap by ~ 3 eV due to its failure in accurately modeling the Zn $3d$ electrons.

In addition to calculation for the band structure of bulk ZnO Ivanov and Pollmann have also carried out an extensive study on the electronic structure of the surfaces of wurtzite ZnO (Ivanov *et al.*, 1981), Using Empirical Tight Binding Method (ETMB) to determine Hamiltonian (eV) for the bulk state, the scattering theoretical method was applied to determine the nature of the surface states. The calculated data was found to be in very good agreement with experimental data obtained from electron loss energy spectroscopy (EELS) and ultra violet photoelectron spectroscopy (UPS). There is a common and simple method for determining of band gap that is base on absorption spectroscopy. For a direct bandgap, the absorption coefficient α is related to light frequency according to the following formula:

$$\alpha = A^* (h\nu - E_g)^{1/2} \quad \text{Eq(1)}$$

$$A^* \approx \frac{q^2 \left(2 \frac{m_h^* m_e^*}{m_h^* + m_e^*} \right)^{3/2}}{n c h^2 m_e^*} \quad \text{Eq(2)}$$



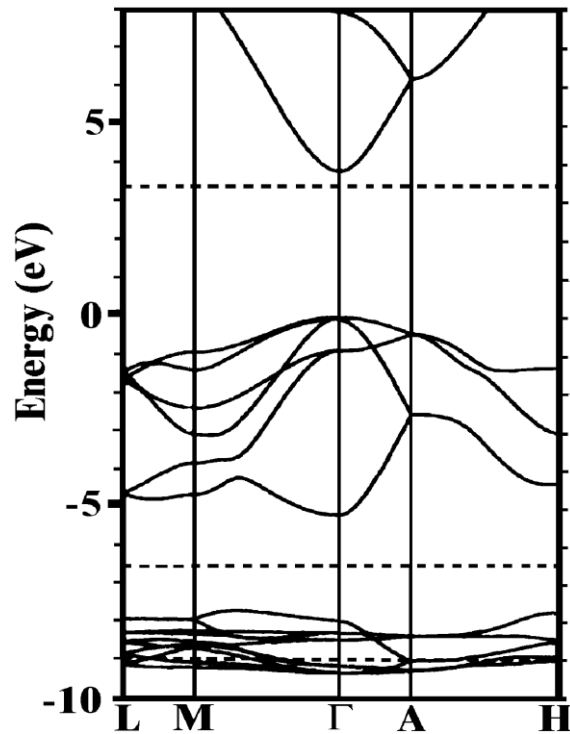


Figure 2: The LDA band structure of bulk wurtzite ZnO calculated using dominant atomic self-interaction-corrected pseudopotentials. Zinc oxide bulk, thin films and nanostructures processing, properties and applications

Where α is the absorption coefficient, a function of light frequency, ν light frequency, h Planck's constant, $h\nu$ the energy of a photon with frequency ν , E_g the band gap energy, A^* a certain frequency-independent constant, with formula above, m_e^* and m_h^* are the effective masses of the electron and hole, q the elementary charge, n the index of refraction and c the light, respectively.

1.2.1 Opportunities from band gap engineering

ZnO has been identified as a promising candidate for UV opto-electronic devices and the main emphasis is on band-gap engineering for the design of ZnO-based short

wavelength transparent opto-electronic devices. In the case of ZnO, alloying with MgO and CdO is an effective means of increasing or decreasing the energy band gap, respectively (Makino and Segawa *et al.*, 2000).

For a semiconductor to be useful, particularly in reference to optoelectronic device, band gap engineering is a crucial step in device development. By allowing the starting semiconductor with another material of different band gap, the band gap of resultant alloy material can be finely tuned, thus affecting the wavelength of exciton emissions.

1.3 Electrical properties

The electrical properties of ZnO are hard to quantify due to large variance of quality of sample available. The background carrier concentration varies a lot according to the quality of layers but is usually $\sim 10^{16} \text{ cm}^{-3}$. The largest reported n-type doping is $\sim 10^{26}$ electrons cm^{-3} and largest reported p-type doping is $\sim 10^{19}$ holes cm^{-3} . However such high levels of p-conductivity are questionable and have not been experimentally verified. The exciton binding energy is 60 meV at 300K, and is one of the reasons why ZnO is so attractive for optoelectronic device applications.

1-4 Optical properties

The optical properties of ZnO are heavily influenced by energy band structure and lattice dynamics. Meyer *et al.*,(2004) had a comprehensive review of the optical properties of excitonic recombination in bulk n-type ZnO .This work gives a comprehensive treatment



and analysis of the excitonic spectra obtained from ZnO, and assign many defect related spectra feature, as well as donor-acceptor pair (DAP) emission. A broad defect related peak extending from ~ 1.9 to ~ 2.8 eV is also a common optical feature of ZnO. Known as the green band, the origin of its luminescence is still not well understood and has in the past been attributed to a variety of different impurities and defects. A broad defect related peak extending from 1.9-2.8 eV is also common optical feature of ZnO, known as the green band, the origin of its luminescence spectra of n type ZnO measured at 4.2 K. The excitonic, DAP and extended green band emission can all be clearly seen, as can the phonon replicas produced from the longitudinal optical phonons (LO).

In terms of more fundamental optical properties of ZnO, there have been a number of comprehensive studies to determine the refractive index and dielectric constant of this material (Yoshigawa *et al.*, 1997). The measurements were all carried out using spectroscopic ellipsometry.

1-5 ZnO nanostructures

Nanostructured ZnO materials have received broad attention due to their distinguished performance in electronic, optics and photonics. With reduction in size, novel electrical, mechanical, chemical and optical properties are introduced, which are largely believed to be the result of surface and quantum confinement effects. Nanowire structures are the ideal system for the studying the transport process in 1D-confined objects, which are of benefit not only for understanding the fundamental phenomena of low dimensional systems, but also for developing new generation nanodevices with high



performance. The lack of center of symmetry in wurtzite, combined with a large electrochemical coupling, results in strong piezoelectric properties and the consequent use of ZnO in mechanical actuator and piezoelectric sensors. In addition ZnO is a wide band gap (3.37eV) compound semiconductor that is suitable for short wavelength optoelectronic applications. The high exciton binding energy (60 meV) in ZnO crystal can ensure efficient excitonic emission at room temperature and room temperature ultraviolet (UV) luminescence has been reported in disordered nanoparticles and thin films. ZnO is transparent to visible light and can be made highly conductive by doping. ZnO is versatile functional material that has a diverse group of growth morphologies such as nanorods, nanobelts, nanowires, nanocages, nanocombs, nanosprings, nanorings and nanohelices (Wang *et al.*, 2001).

1.5.1 Nanorods and nanowires

Growth of 1D nanostructure usually follows the VLS approach, in which a liquid alloy droplet composed of a metal catalyst component (such as Au, Fe) and a nanowire component (such as Si, III–V compound, II–V compound, oxide) is first formed under the reaction conditions. The metal catalyst can be rationally chosen from the phase diagram by identifying metals in which the nanowire component elements are soluble in the liquid phase but do not form solid compounds more stable than the desired nanowire phase. For the 1D ZnO nanowires grown via a VLS process, the commonly used catalyst for ZnO is Au (Yang *et al.*, 2001). The liquid droplet serves as a preferential site for absorption of gas phase reactant and, when supersaturated, the nucleation site for crystallization. Nanowire growth begins after the liquid becomes supersaturated in

